Received: 10 September 2020 | Revised: 29 December 2020 | Accepted: 17 January 2021

DOI: 10.1002/jsp2.1139

RESEARCH ARTICLE

JOR Spine OPEN ACCESS

Preliminary investigation of spinal level and postural effects on thoracic muscle morphology with upright open MRI

Anoosha Pai S[1,2] | Honglin Zhang[3] | John Street[2,4] | David R. Wilson[2,3,4] | Stephen H. M. Brown[5] | Thomas R. Oxland[2,4,6]

[1]School of Biomedical Engineering, University of British Columbia, Vancouver, Canada

[2]ICORD, University of British Columbia, Vancouver, Canada

[3]Centre for Hip Health and Mobility, University of British Columbia, Vancouver, Canada

[4]Department of Orthopaedics, University of British Columbia, Vancouver, Canada

[5]Department of Human Health and Nutritional Sciences, University of Guelph, Guelph, Canada

[6]Department of Mechanical Engineering, University of British Columbia, Vancouver, Canada

Correspondence
Thomas R. Oxland, Professor, Orthopaedics and Mechanical Engineering, University of British Columbia, ICORD, Blusson Spinal Cord Centre at VGH, 3rd Floor, 818 West 10th Avenue, Vancouver, BC V5Z 1M9, Canada.
Email: toxland@icord.org

Funding information
Medtronic Canada; Natural Sciences and Engineering Research Council of Canada, Grant/Award Number: CRDPJ 515076-17; Canadian Institutes of Health Research, Grant/Award Number: 148828

Abstract

Objective: Spinal-muscle morphological differences between weight-bearing and supine postures have potential diagnostic, prognostic, and therapeutic applications. While the focus to date has been on cervical and lumbar regions, recent findings have associated spinal deformity with smaller paraspinal musculature in the thoracic region. We aim to quantitatively investigate the morphology of trapezius (TZ), erector spinae (ES) and transversospinalis (TS) muscles in upright postures with open upright MRI and also determine the effect of level and posture on the morphological measures.

Methods: Six healthy volunteers (age 26 ± 6 years) were imaged (0.5 T MROpen, Paramed, Genoa, Italy) in four postures (supine, standing, standing with 30° flexion, and sitting). Two regions of the thorax, middle (T4-T5), and lower (T8-T9), were scanned separately for each posture. 2D muscle parameters such as cross-sectional area (CSA) and position (radius and angle) with respect to the vertebral body centroid were measured for the three muscles. Effect of spinal level and posture on muscle parameters was examined using 2-way repeated measures ANOVA separately for T4-T5 and T8-T9 regions.

Results: The TZ CSA was smaller (40%, P = .0027) at T9 than at T8. The ES CSA was larger at T5 than at T4 (12%, P = .0048) and at T9 than at T8 (10%, P = .0018). TS CSA showed opposite trends at the two spinal regions with it being smaller (16%, P = .0047) at T5 than at T4 and larger (11%, P = .0009) at T9 than at T8. At T4-T5, the TZ CSA increased (up to 23%), and the ES and TS CSA decreased (up to 10%) in upright postures compared to supine.

Conclusion: Geometrical parameters that describe muscle morphology in the thorax change with level and posture. The increase in TZ CSA in upright postures could result from greater activation while upright. The decrease in ES CSA in flexed positions likely represents passive stretching compared to neutral posture.

KEYWORDS

erector spinae, magnetic resonance imaging, muscle morphometry, paraspinal muscle, thoracic spine, transversospinalis, trapezius, upright MRI

1 | INTRODUCTION

Spinal geometry in upright postures is different than in supine.[1-3] Most symptoms of spinal deformities are worse in a standing posture[4] and upright clinical measurements are important for better diagnosis and treatment outcomes.[5,6] For example, a study in people with low-back pain found that geometric parameters such as lumbosacral angle, lordosis, and disc height were significantly different in upright postures in 70% of patients when compared to their supine measurements.[6] Another study showed that the Cobb angle of the thoracolumbar major curve was significantly higher, and the lumbar lordosis was considerably lower while standing than when measured supine.[2] It is intuitive that with the change in spinal geometry in different postures, the overall morphometry, position, moment-arm and activation levels of the surrounding musculature[7] would also change.

Closed-bore magnetic resonance imaging (MRI) requires the subject to be in a supine or prone position. Our knowledge of muscle morphology is thus restricted to the non-upright postures. This poses a challenge in using the muscle data obtained from clinical imaging in the development of biomechanical spine models, and personalized treatment strategies.[8] Open and upright MRI allows subjects to be imaged in different weight-bearing postures and has shown some encouraging results in visualizing muscles in vivo. Upright imaging studies that focused on the lumbar spine have shown significant changes in muscle morphology between supine and upright postures[9-13] and differences between the flexed and extended positions.[14] In the cervical spine, it was shown that the position of the head and neck significantly affected area and location of the sternocleidomastoid and posterior neck muscles.[15] Almost all upright MRI studies have been on the cervical and lumbar spine. However, spinal extensor muscle strength is shown to be more important for muscular support of the thoracic spine[16,17] and is presumed to have the greater clinical significance with respect to thoracic spinal health.[18,19]

Thoracic hyperkyphosis, an exaggerated anterior curvature of the thoracic spine, is known to affect 20% to 40% of older adults above the age of 60 years,[20] with an average cost of about 54 000 USD for principal diagnosis of spine curvature.[21,22] Previous research has reported that lower muscle density,[23] smaller muscle volume,[24] and reduced extensor muscle strength[16,25-27] in the lumbar spine is associated with kyphosis[16,25-27]. On the other hand, the findings of a recent longitudinal study suggested that smaller cross-sectional area (CSA) and lower density (muscle-to-fat ratio) of the thoracic muscles, especially those situated nearest to the kyphosis curvature was associated with kyphosis severity more than those in the lumbar region.[18]

Some studies have assessed spinopelvic musculature in upright postures while trying to understand the fundamental morphological changes in healthy individuals. Shaikh et al assessed and quantified muscles at three lumbar levels[13] and in the pelvic region in different upright postures. This study follows a similar approach for investigating two paraspinal extensor muscles—erector spinae (ES) and transversospinalis (TS) and one posterior muscle—trapezius (TZ) in the thoracic spine. Although the TZ is mainly involved in stabilizing and controlling the scapula, it has been noted that correction of thoracic kyphosis should be included among exercises designed to achieve normal scapular alignment, which could imply that the TZ may be involved in development of hyperkyphosis.[28,29]

In light of the high prevalence of adult spinal deformities, the incremental cost effectiveness ratio of correction surgery to non-surgical management at 3 year follow-up was estimated as 375 000 USD.[22,30] Proximal junctional kyphosis (PJK) is a well-documented post-surgical clinical problem where understanding the thoracic muscle morphology is relevant. PJK often manifests as a kyphotic change in the disc space of vertebral body adjacent to the fusion.[31] PJK typically occurs in the thoracolumbar junction[32,33] or upper thoracic levels[33-35] and is found to be prevalent in about 17% to 39% of patients[36] who undergo a fusion surgery in the thoracolumbar spine. PJK is attributed to the failure of the soft tissue at the back[22] such as loss of muscle CSA and density,[37] atrophy,[38,39] altered muscle activations,[40] and reduced muscle strength.[38,41] Furthermore, clinical studies by Yagi et al.[42] suggested that 41% of patients post lumbar degenerative scoliosis surgery, developed progressive global kyphosis in the thorax. Clearly, PJK is a multifactorial problem where the health of the surrounding musculature, especially those in the thoracic spine, is important.[43,44]

Given that paraspinal musculature in the thorax plays a vital role in maintaining weight-bearing postures, onset and progression of adult spinal deformity, and post-surgical pathologies, there is a need to quantitatively investigate thoracic musculature in different postures in vivo. Thus, with an aim to fill this literature gap, our study had two objectives. The first objective was to quantitatively investigate the parameters such as CSA and position of muscles in the thoracic region. The second objective was to study the effect of spinal level and posture on these muscle parameters.

While our previous article[45] focused on outlining detailed segmentation guidelines and assessing segmentation repeatability on the thoracic muscle data, this study focuses on investigating the effect of upright, seated, and supine postures on thoracic muscle morphometry.

2 | MATERIALS AND METHODS

2.1 | Study participants

Six healthy participants were recruited (five male and one female, age 26 ± 6 years, height 177 ± 9 cm, and weight 75 ± 10 kg, BMI 24 ± 3 kg/m^2 with no history of spine conditions).

2.2 | Image acquisition

The imaging protocol for human-study was approved by the Clinical Research Ethics Board (CREB) of the University of British Columbia and the Vancouver Coastal Health Research Institute (H10-00942). All the participants signed an informed and written consent along with

permission for publishing their imaging data without disclosing any personal information. The participants were scanned within the 56 cm gap of a 0.5 T vertical open MRI scanner (MROpen, Paramed, Genoa, Italy) using a T1-weighted Gradient Field Echo sequence (TR/TE = 480/8 ms, FOV 24 cm, scan matrix 224*192, slice thickness 4 mm with 0.4 mm gap, NEX = 2, 153 seconds imaging time for each posture). Each volunteer was scanned in four postures: supine, standing upright, standing with 30° forward flexion, and seated 90° flexion from the hips (sit upright) as shown in Figure 1. Consistency in flexed posture across all subjects was achieved by asking each participant to flex forward from their neutral standing posture by a distance equal to the product of approximate length of their torso and sine of the desired angle of flexion (Figure 1E). The seated posture was achieved by seating each subject on the scan table where the backrest was setup 90° relative to its seat (Figure 1F). Owing to the challenges in aligning the thoracic spine to the center of the scanner at higher flexion angles, 30° was chosen as opposed to 45° as typically found in the literature.[13]

Two separate scans were performed for every posture due to the dimensional limitations of the imaging coil and challenges with aligning the same thoracic levels of volunteers with varying heights to the iso center of the MRI scanner for all four postures. Each scan focused on two regions, either T4-T5 (ie, the junction between the upper and the middle thorax), or T8-T9 (ie, the junction between the middle and lower thorax).

The volunteers were systematically repositioned twice in every posture, such that T4-T5 or T8-T9 regions were centered in the scanner. Images were obtained from a stack of continuous, parallel slices (typically 9 or 11 in number) with the middle slice aligned to the center of the intervertebral disc (T4-5 or T8-9) and parallel to it (Figure 2A). The number of slices in a stack was varied in order to cover the entire length of the thoracic regions under consideration.

To accurately detect the required thoracic levels in each region (T4-T5 or T8-T9) in all postures, four fiducial skin markers were placed on the back of the volunteers via manual palpation (Figure 2A).The position of the markers with respect to thoracic vertebral bodies was identified initially with a sagittal localizer scan counting inferior from level C2 in the supine position. The position of these markers was confirmed in upright scans by performing a localizer scan in the seated posture, again counting down from C2. For all scans, the subjects were asked to adopt a relaxed and neutral posture (ie, not slumping or actively extending, or flexing the spine). For comfort and stability, the participants were allowed to rest their hands and hold onto a bar placed in front of them but were instructed to not rely on the bar for any load bearing support. Other bars were positioned at the back of the volunteers and foam spacers were placed on the sides, as an indicator for where to hold a still position, and to avoid side-to-side motion during the scan. To maintain consistency of the scapular position among the subjects and postures, the subjects was asked to hold their shoulders as naturally as possible (not elevated

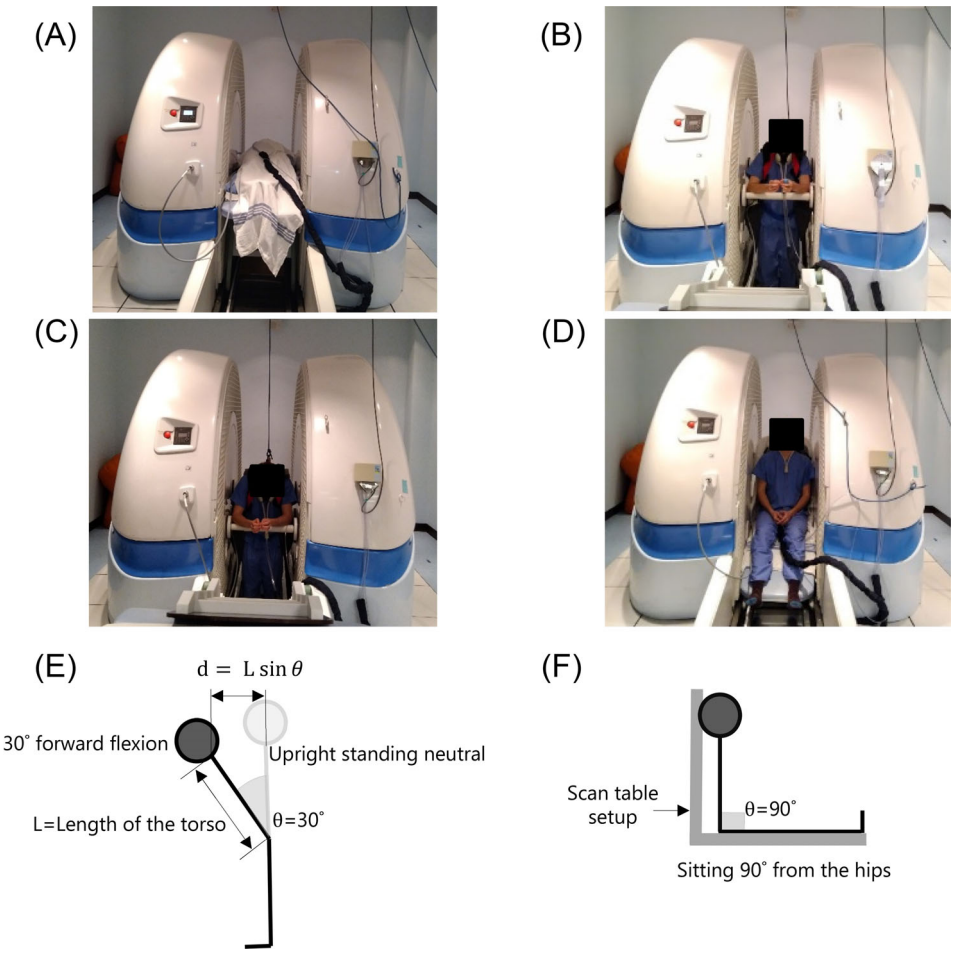

FIGURE 1 MR Open image acquisition for one volunteer in four postures. A, Supine. B, Standing. C and E, Standing with 30° forward flexion. D and F, Seated 90° flexion from the hips (sit upright)

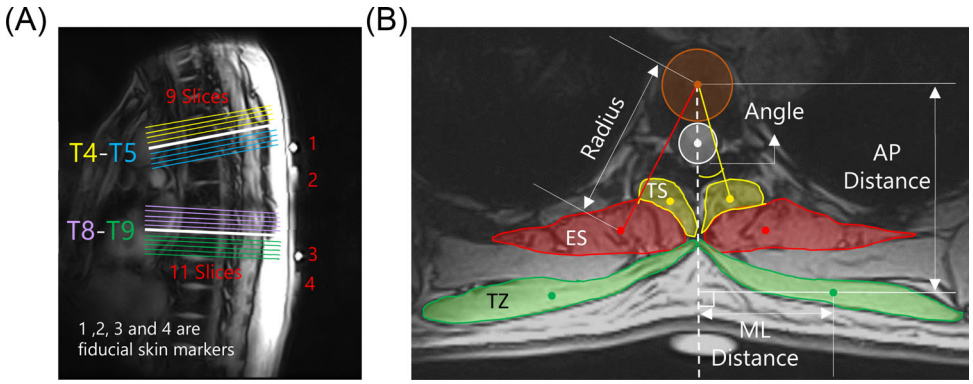

FIGURE 2 A, Sagittal MR image showing the orientation of the parallel slice stack for thoracic regions T4-T5 (9 slices; 4 slices across T4 [yellow], 4 slices across T5 [blue], and 1 mid-disc slice [white]) and T8-T9 (11 slices; 5 slices across T8 [purple], 5 slices across T9 [green] and 1 mid-disc slice [white]) with four fiducial skin markers marked as 1, 2, 3, and 4. B, Image analysis measurements of 2D muscle CSA and position (radius and angle). The brown colored circle represents the vertebral body, the white colored circle represents the vertebral canal, and solid dots represent geometric centroids. AP, anterior–posterior; CSA, cross-sectional area; ES, erector spinae group; ML, medial-lateral; TS, transversospinalis group; TZ, trapezius

upward or extended backward) in upright postures and their arms always positioned adducted to their torso. To prevent the subjects from falling (eg, numbness in the legs, blackouts) in the scanner during upright scans, a safety harness was used connected to a rope suspended from the ceiling (Figure 1B). The rope was slack and does not exert any force on the subject or affect the posture or muscle activations.

2.2.1 | Image analysis

Segmentation guidelines described previously[45] were used to manually segment regions of interest of TZ, ES, and TS in 3D Slicer (Version 4.10.12, http://www.slicer.org).[46] Magnitudes of CSA and positions (radius and angle) were computed as shown in Figure 2B in MATLAB (version R2019a, Natick, Massachusetts: The MathWorks Inc.). CSA (mm^2) was determined by manually tracing the outline of the muscle boundary on every slice, and the centroid was defined as its geometric center. Radius (mm) was measured as the absolute distance between the centroid of the muscle and the vertebral body.[15] Angle, A (degrees) was measured between the line connecting centroids of the muscle and the vertebral body, and the line connecting the centroids of vertebral body and the vertebral canal. Both the vertebral body and the vertebral canal were segmented as circles with constant radii for a given subject as shown in Figure 2B. The anterior-posterior (Radius × cosA) and medial-lateral (Radius × sinA) distances were then computed. Intra and inter-rater repeatability of segmentation for all muscles was generally good/excellent (average Intraclass Correlation Coefficient ICC [3, 1] = 0.9 with ranges of 0.56-0.98).[45]

2.2.2 | Data analysis

Statistical analysis was performed in Statistica (Version 13, Copyright 1984-2017, TIBCO Software Inc.). For analysis, the parameters for the right and left muscles were added for the CSA and were averaged for radius and angle, since no significant effect of side was found for these parameters. Level-specific properties were obtained by taking the averages of each parameter computed on all slices passing through each level (see Figure 2A). The effect of level and posture on CSA, radius, and angle of every muscle was separately evaluated for each thoracic region with a two-way repeated measures analysis of variance (ANOVA) with factors of spinal level and posture. Normality and sphericity of the data were initially confirmed. Statistical significance was considered at $P < .05$. Student-Neuman-Keuls tests were performed for post-hoc analyses and Greenhouse-Geisser correction was applied in cases of violation of sphericity criteria. The Friedman nonparametric test was performed for specific comparisons in case of severe violation of normality criteria. The effect of level and posture was evaluated between T4 and T5, and between T8 and T9.

3 | RESULTS

The effects of level and posture, and any interactions on CSA, radius and angle are presented for each muscle at each thoracic region, with summative data presented in Figures 3, 4, and 5 and Table 1, Tables 2 and 3. Note that posture effects for each thoracic region are presented as averaged across the two spinal levels (Tables 1 and 2), and the spinal level effects are presented as averaged across all four postures (Table 3).

3.1 | Cross-sectional area

3.1.1 | Trapezius

The CSA of TZ was found to be 40% ($P = .0027$) larger at T8 compared to T9 (Figure 3A), while no significant level effect was observed between T4 and T5. Posture significantly ($P = .0001$) affected the CSA at T4-T5 region with an increase of approximately 10%, 12%, and 23% in standing, flexed and sitting postures when compared to supine (Figure 3A and

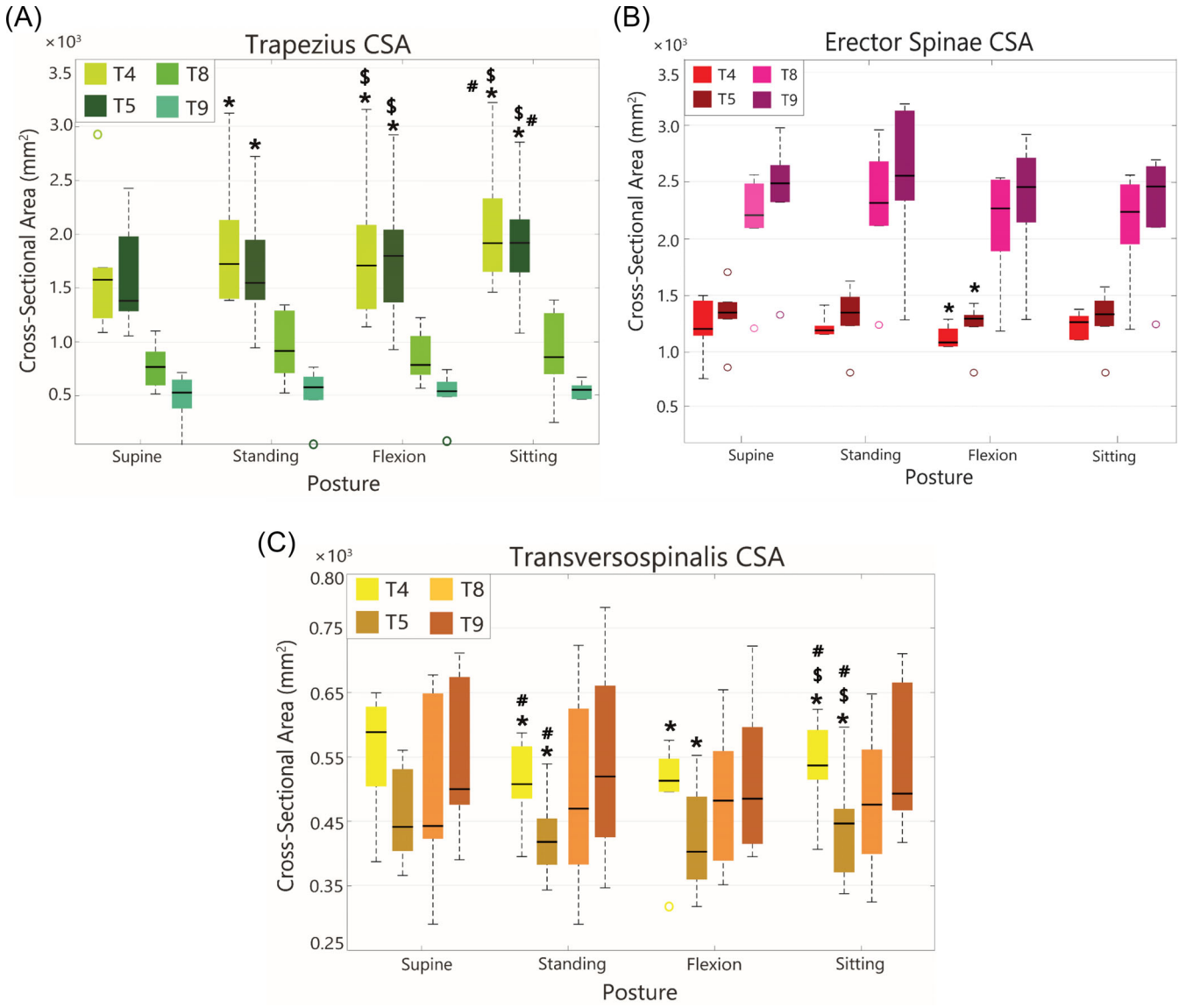

FIGURE 3 Box plots of muscle CSA (averaged across all subjects) shown for each posture by spinal level. The median is marked by the horizontal line inside the box, the ends of the box are the upper and lower quartiles, and the whiskers are the two lines outside the box that extend to the highest and lowest observation. Outliers are represented by circular markers above or below each box. Post hoc significant marked by notations. * = significant from supine, $ = significant from standing, # = significant from flexion. CSA, cross-sectional area

Figure 5). The CSA also was 10% and 9% lower in the standing and flexion postures compared to sitting. At T8-T9 region, however, CSA did not significantly vary with posture. For the number of specimens tested, no level-posture interaction was observed for TZ CSA.

3.1.2 | Erector spinae

Significant level effects were observed for ES CSA across both the spinal regions. The CSA was larger by 12% (P = .0048) and 10% (P = .0018) at T5 than T4 and at T9 than T8, respectively (Figure 3B). For posture, no significant changes were detected at T8-T9 region. At T4-T5 region, the CSA decreased by 10% (P = .0508) in flexion when compared to supine (Figure 3B and Figure 5). No interaction was detected between levels and postures at T4-T5, but significant interaction was detected at the lower thoracic region, T8-T9 (P = .0052). Specifically, at level T8, there was 7%, 8%, and 7% decrease in CSA for supine, flexed and sitting compared to standing. At level T9, there was 3% increase, 4% and 6% decrease for standing, flexed and sitting respectively compared to supine, and a 7% and 9% decrease for flexion and sitting compared to standing.

3.1.3 | Transversospinalis

TS CSA showed opposite trends at the two regions under consideration. The CSA was 16% (P = .0047) smaller at T5 than the T4 level (Figure 3C and Figure 5), but it was larger by about 11% (P = .0009)

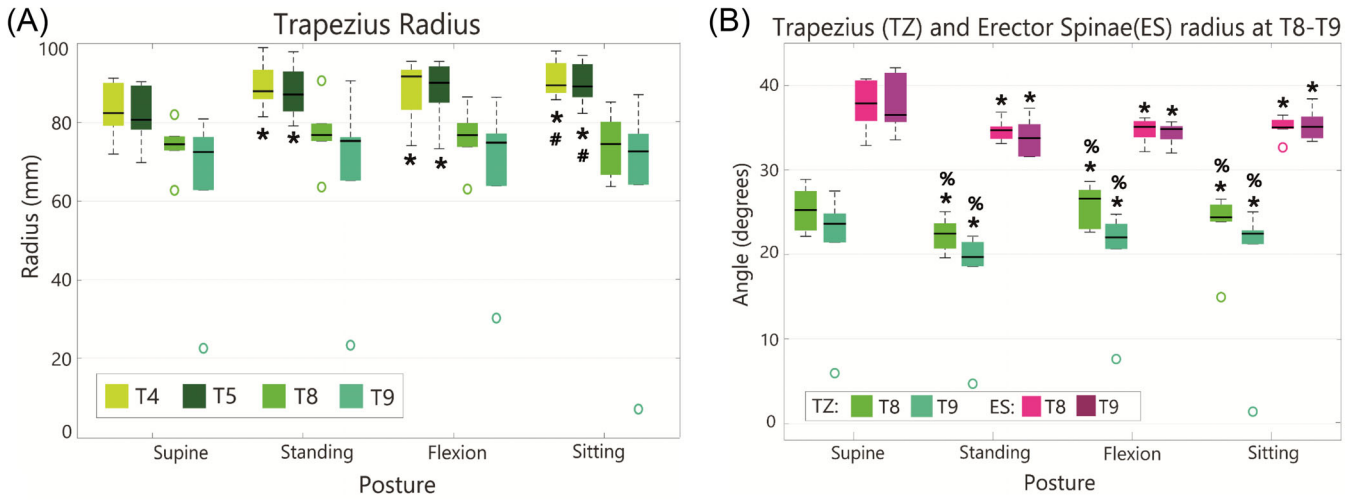

FIGURE 4 A, Box plots of TZ Radius shown for each posture (averaged across all subjects) by level. B, Box plots of TZ and ES angle (averaged across all subjects) shown for each posture at region T8-T9. The median is marked by the horizontal line inside the box, the ends of the box are the upper and lower quartiles, and the whiskers are the two lines outside the box that extend to the highest and lowest observation. Outliers are represented by circular markers above or below each box. Post hoc significant marked by notations. * = significant from supine, $ = significant from standing, # = significant from flexion % = results from nonparametric Friedman test

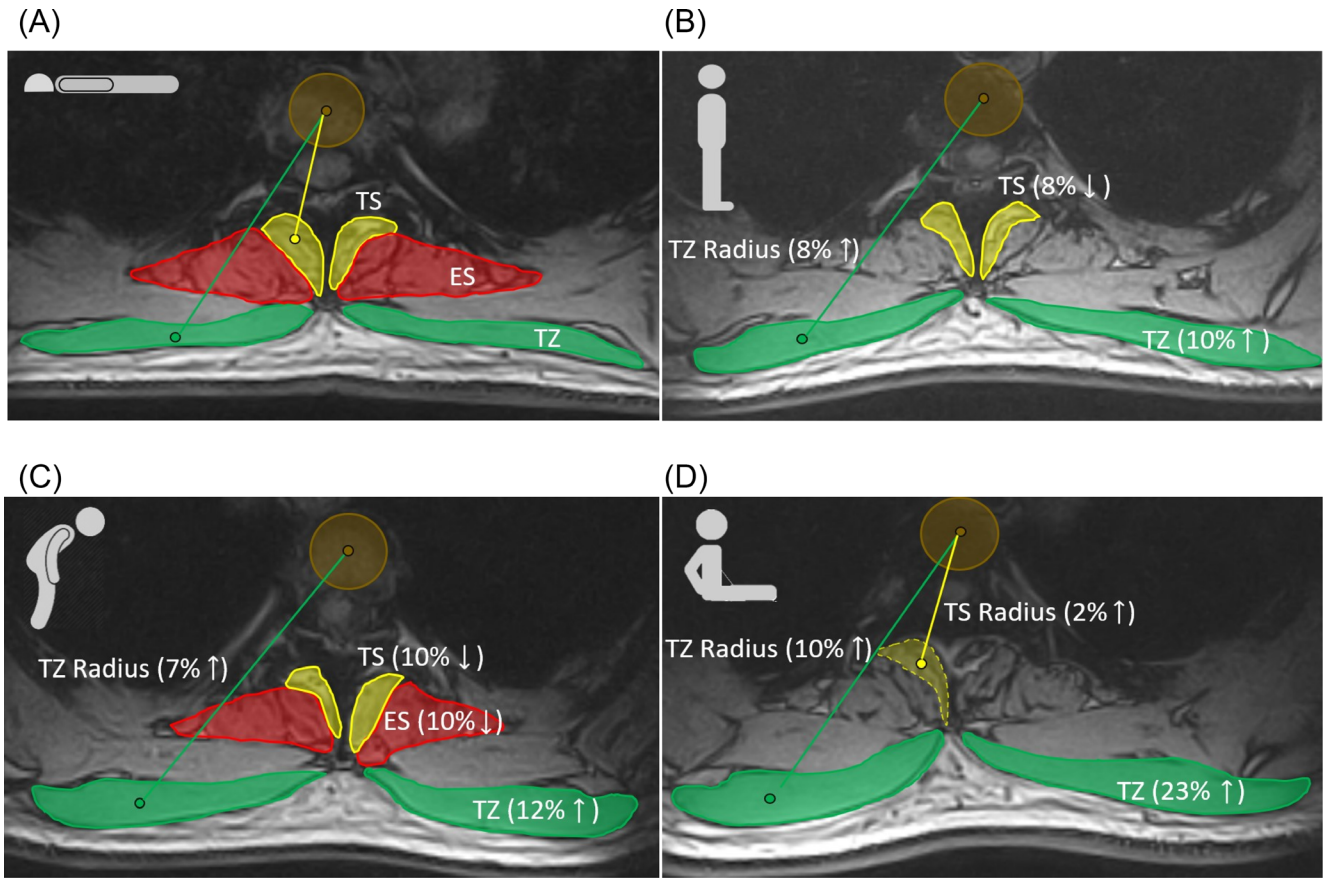

FIGURE 5 Sample illustration at level T4 showing post hoc significant for CSA, radius and angle in upright postures with respect to supine as reference. A, supine. B, upright standing. C, forward flexion. D, upright sitting. CSA, cross-sectional area; ES, erector spinae group; TS, transversospinalis group; TZ, trapezius

(Figure 3C) at T9 than the T8 level. Although posture did not seem to have any effect on CSA at T8-T9, there was an 8% and 10% decrease in upright standing and flexion when compared to supine, a 2% decrease and 7% increase in standing and sitting compared to flexion at T4-T5 (P = .0019). The interactions between level and posture were found to be not significant for our data.

TABLE 1 Average muscle cross-sectional area (CSA in mm^2), radius (mm), and angle (degrees) for all subjects across different postures (averaged across levels T4 and T5). Significant results ($P < .05$) from Neuman Keuls post-hoc indicated by symbols in legend. The CSA value is the sum of right and left sides. The radius and angle values are averages of right and left sides

		CSA (mm^2)		Radius (mm)		Angle (deg)	
Muscle	Posture	Average	SD	Average	SD	Average	SD
TZ	Supine	1633	573	82	7	36	7
	Standing	1800[a]	626	89[a]	6	36	2
	Stand 30F	1831[a]	696	88[a]	8	39	5
	Sitting	2005[a,b,c]	596	90[a,c]	5	38	4
ES	Supine	1306	266	59	4	31	3
	Standing	1266	254	59	4	31	3
	Stand 30F	1177[a]	219	59	4	32	3
	Sitting	1260	263	60	4	32	3
TS	Supine	508	83	43	2	16	2
	Standing	468[a,c]	65	44	3	15	3
	Stand 30F	458[a]	83	44	3	15	2
	Sitting	490[b,c]	80	44[a]	3	15	2

Note: 30F represents 30° forward flexion posture.
Abbreviations: CSA, cross-sectional area; ES, erector spinae group; SD, standard deviation; TS, transversospinalis group; TZ, trapezius.
[a]Significant from supine.
[b]Significant from standing.
[c]Significant from flexion.

TABLE 2 Average muscle cross-sectional area (CSA in mm^2), radius (mm), and angle (degrees) across the different postures (averaged across levels T8 and T9). Significant results ($P < .05$) from Neuman Keuls post-hoc indicated by symbols in legend. The CSA value is the sum of right and left sides. The radius and angle values are averages of right and left sides

		CSA (mm^2)		Radius (mm)		Angle (deg)	
Muscle	Posture	Average	SD	Average	SD	Average	SD
TZ	Supine	707	114	72	4	25	2
	Standing	740	268	72	14	20[a,b]	4
	Stand 30F	689	229	72	12	23[a,b]	4
	Sitting	684	319	69	18	21[a,b]	7
ES	Supine	2299[a]	225	72	3	40[a]	1
	Standing	2422[a]	575	71	7	34[a,b]	2
	Stand 30F	2244[a]	491	69	7	35[a,b]	1
	Sitting	2227[a]	474	70	6	35[a,b,c]	2
TS	Supine	463	65	48	1	14	1
	Standing	513	147	48	4	13	2
	Stand 30F	498	117	47	4	13	2
	Sitting	501	118	48	4	13	1

Note: 30F represents 30° forward flexion posture.
Abbreviations: CSA, cross-sectional area; ES, erector spinae group; SD, standard deviation; TS, transversospinalis group; TZ, trapezius.
[a]Results from nonparametric Friedman test.
[b]Significant from supine.
[c]Significant from standing.

3.2 | Muscle positions (radius and angle)

3.2.1 | Trapezius

The TZ radius was consistently higher at level T4 than at T5 ($P = .0097$) (Figure 4A), although the magnitude was small (~1%). However, no significant difference was found between levels T8 and T9. On the other hand, the angular position was found to be consistent across T4 and T5 levels, while the angle was 18% ($P = .0143$, Friedman test) larger at T8 than at T9 (Figure 4B). For postures, the radius at T4-T5 for standing, flexion and sitting was respectively 8%, 7% and 10% more than that in supine, and was 2% more in sitting than in flexion ($P = .0005$) Figure 4A). The angle at T8-T9 was 21%, 10%, and 16% smaller in standing, flexion and sitting compared to

TABLE 3 Average muscle cross-sectional area (CSA in mm^2), radius (mm), and angle (degrees) for all subjects across T4, T5, T8, and T9 levels (averaged for all postures). Significant results ($P < .05$) from Neuman Keuls post-hoc indicated by symbols in legend. The CSA value is the sum of right and left sides. The radius and angle values are averages of right and left sides

		CSA (mm^2)		Radius (mm)		Angle (deg)	
Muscle	Level	Average	SD	Average	SD	Average	SD
TZ	T4	1883	640	88[a]	7	37	5
	T5	1751	575	87	7	37	5
	T8	881[b]	282	75	7	25[b,c]	3
	T9	529	208	67	20	20	7
ES	T4	1184[a]	232	59	4	31	3
	T5	1321	251	59	4	32	3
	T8	2184[b]	449	70[b]	6	36	3
	T9	2413	509	71	5	36	3
TS	T4	524[a]	82	44	3	15[a]	2
	T5	438	78	44	3	15	2
	T8	467[b]	111	47	4	14[b]	2
	T9	520	110	48	3	13	1

Abbreviations: CSA, cross-sectional area; ES, erector spinae group; TS, transversospinalis group; TZ, trapezius; SD, standard deviation.
[a]significant between levels T4 and T5.
[b]Significant between levels T8 and T9.
[c]Results from nonparametric Friedman test.

supine ($P = .0056$). For the number of samples analyzed, both position parameters showed no significant level-posture interactions across both levels.

3.2.2 | Erector spinae

While there were no level-effects observed between T4 and T5 for both radius and angle, the ES radius at T9 was always found to be larger than at T8 ($P = .0156$), but the magnitude of difference was negligible (~1%). While radius did not vary with posture at both spinal levels and the ANOVA showed no interaction between levels and posture for the given dataset, the angle decreased by about 12% at T8 and about 14% at T9 from supine to all upright postures. The angle between stand to sit significantly increased at T9, with a small difference in magnitude (~4%) Figure 4B).

3.2.3 | Transversospinalis

No significant level-effects were noted in TS radius across both thoracic regions. However, the angles at T4 and T8 were larger by ~3% ($P = .0405$) and ~8% ($P = .0073$) as compared to levels T5 and T9 respectively. For posture effects, the radius showed a small increase (~2%) from supine to sitting from T4-T5 ($P = .0272$) and no significant changes from T8-T9 region. For the number of samples analyzed, angle showed no significant effects of posture, and both radius and angle showed no posture-level interactions.

4 | DISCUSSION

The CSA and position of three muscles were quantitatively investigated at two levels in the thoracic spine. The effect of thoracic level and posture on the muscle parameters was also examined.

4.1 | Comparison with literature

The magnitudes of CSAs reported this study (Table 4) were overall larger than those reported in previous studies,[18,47] but still within one SD. The reasons for these differences could be multifold. First, the McGill et al.[47] study only considered longissimus thoracis, iliocostalis lumborum (from ES), and multifidus (from TS) while computing the paraspinal muscle CSA, while our study also considered spinalis in the ES, and semispinalis and rotatores in TS group. Second, considerable intermuscular gaps were found between spinalis and longissimus within the ES group, and between ES and TS functional groups, which were included in the region-of-interest of paraspinal muscle CSA.[45] Third, in the study by Lorbergs et al,[18] all the subjects were considerably older (mean age: 61 years) and had a higher BMI (27.5 kg/m^2) than the volunteers in our study. It is intuitive that CSA reduces in size with increase in age due to age-related atrophy and physiological changes. In addition, the CSA reported from Lorbergs et al[18] study was measured at the T7-T8 disc, while the our study reported data at T8 and T9 levels. Also, since no other studies, to the best of our knowledge, have reported CSA values at the T4 level, we have not made any direct comparison.

The radius and angles measured in this study essentially give the anterior-posterior (A-P) and medial-lateral (M-L) distances from the vertebral body center, which is also a conventional approach for comparing relative position of a muscle in axial radiographs.[48-56] These magnitudes were comparable with the values reported in previous work[48,53,56] and found to lie within one SD as seen from Tables 5 and 6. The variations observed, however, could have been due to the differences in the sampled population. The subjects in the Kumar et al.[53] study were older (58.6 year) but had similar BMI (25.9 kg/m^2) as that of the volunteers in this study. This may indicate that with increasing age, CSA decreases, thereby decreasing the distance of muscle from the vertebral body.

4.2 | Trends due to level and posture

Most observed changes in thoracic muscle CSA were expected due to the muscle anatomy. While, the large difference (40%) in CSA for TZ from T8 to T9 characterizes its tapering,[45,57] a large SD (Table 2) is indicative of wide variation in insertion points along lower thoracic levels (T8 to T12).[45,58] In addition, paraspinal muscle (especially ES in the entire spinal column and multifidus in the thoracolumbar and lumbar region) size is known to typically increase caudally[45,58,59] and a similar trend was observed in our study (Table 3 and Figure 3B).

The increase (up to 23%) in TZ CSA at T4-T5 region in upright postures when compared to supine could be due to muscle activation in upright postures. Our results, however, showed a decrease (about 10%) in CSA during upright flexion compared to erect seated position, which is contrary to the findings in the literature,[60] where substantial activation was observed in the middle and lower TZ in the slouched sitting compared to sitting erect. While TZ is known to hyperactivate during slouching, we acknowledge the possibility of these muscles undergoing passive stretching during torso flexion.[61] Passive stretching is a concurrent effect of the lengthening of the muscles, a mechanical behavior of transverse contraction during longitudinal stretching, which is expected for any typical elastic material or tissue. Furthermore, the head/neck posture was not controlled in our study and could also affect the CSA measures of TZ. Further investigation on the muscle activation levels in different postures is required to accurately validate our assertion.

O'Sullivan et al.[62] showed that the superficial lumbar multifidus and thoracic ES muscles are more active in maintaining optimally aligned, erect postures, than during the adoption of passive postures. Although ES and TS are extensor muscles, which act to maintain more active extended postures, the decrease in CSA in upright standing (~8% for TS at T8-T9) compared to supine or sitting could be due to the fact that the participants in our study may have adopted a slightly slouched and comfortable upright posture since they were not instructed to hold an active and erect trunk. Furthermore, the decrease in CSA at both regions going from neutral to flexed posture could be attributed to passive stretching, which aligns with the findings for lumbar ES and multifidus.[61] Moreover, the significant level-posture interaction suggests that activation may not be uniform throughout the length of the muscle and is level and posture dependent.

Thoracic spine position is known to significantly affect scapular kinematics,[29] where the scapula is more elevated and protracted in a slouched posture with a smaller posterior tilt when compared to neutral posture. The increase in radius of TZ observed (up to 10%) from supine to flexion may indicate activation of the middle fibers to retract the scapula,[63] while the decrease in angle (up to 21%) at T8-T9 could account for lower thoracic fibers inferiorly acting on scapular elevation. The thoracic fibers of the lumbar ES largely run parallel to the trunk[64] and therefore their orientation with respect to the trunk

TABLE 4 Raw cross-sectional areas (mm^2) (SD in parentheses) of paraspinal muscles measured directly from the MRI scans for supine. PS, paraspinal muscle, includes both ES and TS groups. PO, posterior muscles, includes ES, TS, and TZ groups EM, erector mass, includes longissimus thoracis, iliocostalis lumborum, and multifidus, R, right, L, left

		Average CSA (mm^2) (SD in parentheses)							
Levels		T4		T5		T8		T9	
Side	Muscles	R	L	R	L	R	L	R	L
This study	TZ	851 (360)	829 (372)	800 (296)	785 (279)	406 (113)	376 (135)	259 (141)	221 (127)
	ES	628 (186)	617 (121)	678 (166)	689 (155)	1092 (273)	1067 (273)	1209 (314)	1198 (316)
	TS	283 (52)	274 (63)	236 (36)	222 (41)	237 (66)	251 (99)	273 (78)	268 (61)
	PS	911 (214)	891 (186)	914 (183)	911 (176)	1329 (333)	1318 (361)	1483 (385)	1466 (364)
	PO	1762 (549)	1720 (496)	1714 (470)	1695 (406)	1736 (373)	1694 (414)	1742 (320)	1687 (365)
McGill et al[56]	EM	–	–	743 (70)	675 (78)	1049 (120)	1129 (100)	1413 (304)	1471 (351)
Lorbergs et al[18] averaged for males and females computed at T7-T8 disc	PS					741 (148)			
	PO					1112 (212)			

Abbreviations: CSA, cross-sectional area; ES, erector spinae group; TS, transversospinalis group; TZ, trapezius.

TABLE 5 Anterior-posterior distances (mm) (SD in parentheses) of paraspinal muscles measured directly from the MRI scans for supine. PS, paraspinal muscle, includes both ES and TS groups. EM, erector mass, includes longissimus thoracis, iliocostalis lumborum, and multifidus. R, right, L, left

Levels		Average anterior-posterior distance (mm) (SD in parentheses)							
		T4		T5		T8		T9	
Side	Muscles	R	L	R	L	R	L	R	L
This study	ES	50(4)	50(4)	50(4)	51(3)	56(3)	57(2)	58(3)	57(3)
	TS	42(3)	42(3)	41(3)	42(3)	45(3)	46(2)	46(2)	46(3)
	PS	46(3)	47(4)	47(3)	47(3)	53(3)	53(2)	54(2)	54(3)
McGill et al[56]	EM	–	–	50(3)	50(3)	52(3)	51(3)	52(3)	51(3)
Kumar et al,[53] averaged for males and females at T7	ES	–	–	–	–	49(4)		–	–
	TS	–	–	–	–	48(5)		–	–
Jorgenson et al[48] averaged for males and females	PS					48(3)	46(4)	49(4)	46(4)

TABLE 6 Medial-lateral distances (mm) (SD in parentheses) of paraspinal muscles measured directly from the MRI scans for supine. PS, paraspinal muscle, includes both ES and TS groups. EM, erector mass, includes longissimus thoracis, iliocostalis lumborum, and multifidus. Positive and negative distance corresponds to right and left side of the vertebral body, respectively. R, right, L, left.

Levels		Average medial-lateral distance (mm) (SD in parentheses)							
		T4		T5		T8		T9	
Side	Muscles	R	L	R	L	R	L	R	L
This study	ES	31 (3)	−30(5)	33(4)	−33(6)	44(5)	−43(4)	43(4)	−44(4)
	TS	13(2)	−11(2)	12(2)	−10(1)	12(1)	−11(1)	11(1)	−11(1)
	PS	21 (2)	−19(3)	21(3)	−20(3)	26(2)	−25(2)	25(2)	−25(2)
McGill et al[56]	EM	–	–	27(2)	−27(6)	31(7)	−33(6)	32(4)	−35(4)
Kumar et al,[53] averaged for males and females at T7	ES	–	–	–	–	35(7)		–	–
	TS	–	–	–	–	10(2)		–	–
Jorgenson et al[48] averaged for males and females	PS	–	–	–	–	29(3)	−30(4)	30(3)	−31(3)

(or the vertebral body) remains parallel and is less likely to be affected by changes in orientation of the spine. For example, during flexion (stand to flex) or extension (stand to sit), little or no change (1%) in the radius is noted as compared to supine. Furthermore, thoracic multifidi of the TS group, are known to be more adapted to produce movements in the transverse plane (twisting), with smaller tension and lower amplitude than lumbar multifidus.[65] Thus, the extent of change in radii measured for TS in different postures was negligible (1%), as the postures selected in this study constitutes mainly of sagittal plane movements.

4.3 | Biomechanical modeling implications

Musculoskeletal modeling requires information on muscle parameters such as CSA, moment-arms and relative positions of muscles with respect to the bony anatomy and with respect to each other. Studies have reported such muscle parameters based on in vivo imaging for the lumbar[48,49,52,64,66,67] and cervical spine,[15,68-71] and our study tries to fill the gaps that remain with regards to the thoracic spine, especially in upright postures.

The application of our data to biomechanical spine modeling could be multifold. First, the radius and angle parameters computed here could provide details of curved and wrapped muscle path along the thoracic spine in different postures facilitating more accurate models. Furthermore, changing trends of muscle parameters with different postures could provide crucial information for developing and validating functionally upright thoracic spine models.[7,72]

Second, the data could also aid in validating and explaining the simulated results from models. For example, a lumbar model by Bogduk et al.[64] showed that the overall lengths of lumbar ES and multifidus fascicles increased in the range of 15% to 59% in flexion when compared to upright standing. Knowing that skeletal muscles are isovolumetric, an increase in length would result in corresponding decrease in CSA. Imaging studies on the lumbar muscles confirmed this trend by observing a decrease in CSA during flexion by up to 19%[13] and 28%.[61] Similarly, parallels can be drawn for the thoracic spine, where a 10% decrease in CSA, as observed in our study, could roughly correspond to about a 10% increase in muscle length during flexion. Furthermore, another lumbar imaging study[61] showed that level specific CSAs decreased by different amounts at different

lumbar levels during flexion, suggesting that the lengthening may not be uniform throughout the muscle. A similar trend in CSA is also observed in our study, which could be a crucial takeaway on paraspinal muscle behavior.

Third, our data could be suitably modified based on the approach suggested by McGill et al[56] to get anatomical CSA (ACSA) and moment-arm estimates. For more cylindrical and elongated muscles such as the ES and TS, modified moment-arm values thus approximated could be used the models. However, for a relatively flat and spread out muscle like the TZ, the distances computed in our study could be used for modeling muscle geometry and positions as opposed to computing muscle torques.

4.4 | Clinical implications

Paravertebral muscle size and health was found to have a crucial influence on standing and walking in adults, post-surgery for spinal deformity correction.[73] Reference dataset of thoracic muscle morphology in healthy individuals becomes essential for comparing and analyzing pathological muscle health in a deformity cohort, such as correlating relative sizes of muscles in an individual to functionality or severity of deformity. Our data could also aid in validating future EMG or functional MRI studies performed to improve understanding of muscle activations in different posture in healthy individuals. Furthermore, knowledge of normal muscle behavior in supine vs upright positions could provide valuable insights into identifying and differentiating pathological behavior, especially in asymptomatic spinal conditions. Last, a fundamental understanding of the thoracic muscle morphological changes could eventually lead to clinical insights on the role of muscle and postures in causation of age-related sagittal balance disorders and post-surgical pathologies.

4.5 | Limitations of the study

Interpretation of the data presented in this study must acknowledge the study's limitations. The small sample size of six individuals may influence the observed level and postural trends on the muscle parameters. While thoracic hyperkyphosis is more common in elderly women, our data (healthy and male-dominated) might not be suitable to make direct comparisons with the deformity cohort. We also acknowledge the small sample size being a shortcoming for using our data as normative muscle data representing the healthy cohort. Furthermore, the subjects were asked to hold postures as naturally as possible without exerting load on the support bars and hence muscle activations were not controlled for or measured during this study. Also, due to the restricted field of view of the imaging coil, the muscle could not be imaged along its entire length, which would give more compelling information on changes in muscle belly length with posture. Because of the low-field strength (0.5 T) of the MR scanner, the individual muscles in the group could not be differentiated and the muscle lines-of-action could not be distinguished. Hence, computing ACSA estimates from the MRI CSA as described earlier might require additional computations of muscle line-of-action for upright postures, which is ongoing work in our group. Last, the usage of data reported in this study in computational models might come with biases favoring young and healthy Caucasian males.

5 | CONCLUSION

Overall, this work provides quantitative data on thoracic musculature in healthy individuals thus contributing to the growing spinal muscle literature. It also delivers novel insights into muscle morphometric changes with level and posture, which could potentially aid in developing functionally upright spine models for more accurate simulations and aid in improved clinical support decisions.

ACKNOWLEDGMENTS

The authors thank the Natural Sciences and Engineering Research Council of Canada (NSERC, Project Grant no. CRDPJ 515076-17), Canadian Institutes of Health Research (CIHR, Project Grant no. 148828) and Medtronic Canada for funding this work. The authors are also thankful to James Zhang and Shannon Jennifer Patterson, technologists at the MROpen facility, who have helped in scanning the volunteers.

CONFLICT OF INTEREST

The authors declare that they have no conflict of interest.

AUTHOR CONTRIBUTIONS

Anoosha Pai S conceptualized the overall work, performed the imaging, data and statistical analysis. Honglin Zhang assisted in image protocol development and numerical analysis. John Street provided clinical perspectives. David R. Wilson provided resources for imaging and helped shape the research. Stephen M. Brown provided critical technical feedback and guidance. Thomas R. Oxland provided overall direction and guidance, assisted in data analysis. Anoosha Pai S took the lead in writing the manuscript, with inputs from all authors.

ORCID

Thomas R. Oxland https://orcid.org/0000-0003-3556-6525

REFERENCES

1. Hasegawa K, Okamoto M, Hatsushikano S, Caseiro G, Watanabe K. Difference in whole spinal alignment between supine and standing positions in patients with adult spinal deformity using a new comparison method with slot-scanning three-dimensional X-ray imager and computed tomography through digital reconstructed radiog. *BMC Musculoskelet Disord*. 2018;*5*(1):1-11.
2. Meakin JR, Gregory JS, Aspden RM, Smith FW, Gilbert FJ. The intrinsic shape of the human lumbar spine in the supine, standing and sitting postures: characterization using an active shape model. *J Anat*. 2009;*215*(2):206-211.
3. Wood KB, Kos P, Schendel M, Persson K. Effect of patient position on the sagittal-plane profile of the thoracolumbar spine. *J. Spinal Disord*. 1996;*9*(2):165-169.

4. Toyone T, Toyone T, Tanaka T et al. Changes in vertebral wedging rate between supine and standing position and its association with back pain: a prospective study in patients with osteoporotic vertebral compression fractures. *Spine (Phila. Pa. 1976)*. 2006;*31*(25):2963-2966.
5. Yazici M, Acaroglu ER, Alanay A, Deviren V, Cila A, Surat A. Measurement of vertebral rotation in standing versus supine position in adolescent idiopathic scoliosis. *J Pediatr Orthop*. 2001;*21*(2):252-256.
6. Tarantino U, Fanucci E, Iundusi R, et al. Lumbar spine MRI in upright position for diagnosing acute and chronic low back pain: statistical analysis of morphological changes. *J Orthop Traumatol*. 2013;*14*(1):15-22.
7. McGill SM, Juker D, Axler C. Correcting trunk muscle geometry obtained from MRI and CT scans of supine postures for use in standing postures. *J. Biomech*. 1996;*29*(5):643-646.
8. Dao TT, Pouletaut P, Lazáry Á, Tho MCHB, Ho C, Tho B. Multimodal medical imaging fusion for patient specific musculoskeletal modeling of the lumbar spine system in functional posture. *J Med Biol Eng*. 2017;*37*(5):739-749.
9. Schmid MR, Stucki G, Duewell S, Wildermuth S, Romanowski B, Hodler J. Changes in cross-sectional measurements of the spinal canal and intervertebral foramina as a function of body position: in vivo studies on an open-configuration MR system. *American Journal of Roentgenology*. 1999;*172*:1095-1102.
10. Weishaupt D, Schmid MR, Zanetti M et al. Positional MR imaging of the lumbar spine: does it demonstrate nerve root compromise not visible at conventional MR imaging? *Radiology*. 2000;*215*(1):247-253.
11. Zamani AA, Moriarty T, Hsu L, et al. Functional MRI of the lumbar spine in erect position in a superconducting open-configuration MR system: preliminary results. *J Magn Reson Imaging*. 1998;*8*:1329-1333.
12. Bailey JF, Miller SL, Khieu K et al. From the international space station to the clinic: how prolonged unloading may disrupt lumbar spine stability. *Spine J*. 2018;*18*(1):7-14.
13. Shaikh N, Zhang H, Brown SHM et al. The effect of posture on lumbar muscle morphometry from upright MRI. *Eur Spine J*. 2020;*29*(9):2306-2318.
14. Weishaupt D, Boxheimer L. Magnetic resonance imaging of the weight-bearing spine. *Sem Musculoskeletal Radiol*. 2003;*7*(4):277-286.
15. Stemper BD, Baisden JL, Yoganandan N, Pintar FA, Paskoff GR, Shender BS. Determination of normative neck muscle morphometry using upright MRI with comparison to supine data. *Aviat Sp Environ Med*. 2010;*81*(9):878-882.
16. Sinaki M, Itoi E, Rogers JW, Bergstralh EJ, Wahner HW. Correlation of back extensor strength with thoracic kyphosis and lumbar lordosis in estrogen-deficient women. *Am J Phys Med Rehabil*. 1996;*75*(5):370-374. https://doi.org/10.1097/00002060-199609000-00013
17. Kado DM. The rehabilitation of hyperkyphotic posture in the elderly. *Eur J Phys Rehabil Med*. 2009;*45*(4):583-593.
18. Lorbergs AL, Allaire BT, Yang L et al. A longitudinal study of trunk muscle properties and severity of thoracic kyphosis in women and men: the Framingham study. *J Gerontol Ser A*. 2019;*74*(3):420-427.
19. Crawford RJ, Cornwall J, Abbott R, Elliott JM. Manually defining regions of interest when quantifying paravertebral muscles fatty infiltration from axial magnetic resonance imaging: a proposed method for the lumbar spine with anatomical cross-reference. *BMC Musculoskeletal Disord*. 2017;*18*(1):1-11.
20. Ames CP, Scheer JK, Lafage V, et al. Adult spinal deformity: epidemiology, health impact, evaluation, and management. *Spine Deform*. 2016;*4*(4):310-322.
21. "Healthcare Cost and Utilization Project (HCUP). HCUP Facts and Figures: Statistics on Hospital-based Care in the United States.," 2010. http://www-ncbi-nlm-nih-gov.ezproxy.library.ubc.ca/books/NBK52994.
22. O'Lynnger TM, Zuckerman SL, Morone PJ, Dewan MC, Vasquez-Castellanos RA, Cheng JS. Trends for spine surgery for the elderly: implications for access to healthcare in North America. *Neurosurgery*. 2015;*77*(4):S136-S141.
23. Katzman WB, Cawthon P, Hicks GE, Vittinghoff E, Shepherd J, Cauley JA. Association of spinal muscle composition and prevalence of hyperkyphosis in healthy community-dwelling older men and women Wendy. *J Gerentol*. 2012;*67A*(2):191-195.
24. Katzman WB, Miller-martinez D, Marshall LM, Lane NE, Kado DM. Kyphosis and paraspinal muscle composition in older men: a cross-sectional study for the osteoporotic fractures in men (MrOS) research group. *BMC Musculoskeletal Disord*. 2014;*15*(1):1-9.
25. Itoi E, Sinaki M. Effect of Back-strengthening exercise on posture in healthy women 49 to 65years of age. *Mayo Clin Proc*. 1994;*69*(11):1054-1059.
26. Katzman WB, Sellmeyer DE, Stewart AL, Wanek L, Hamel KA. Changes in flexed posture, musculoskeletal impairments, and physical performance after group exercise in community-dwelling older women. *Arch Phys Med Rehabil*. 2007;*88*(2):192-199.
27. Benedetti MG, Berti L, Presti C, Frizziero A, Giannini S. Effects of an adapted physical activity program in a group of elderly subjects with flexed posture: clinical and instrumental assessment. *J Neuroeng Rehabil*. 2008;*5*:32. https://dx.doi.org/10.1186/1743-0003-5-32.
28. Yoo W. Effects of thoracic posture correction exercises on scapular position. *J Phys Ther Sci*. 2018;*30*(3):411-412.
29. Kebaetse M, Mcclure P, Pratt NA. Thoracic position effect on shoulder range of motion, strength, and three-dimensional scapular kinematics. *Arch Phys Med Rehabil*. 1999;*80*:945-950.
30. McCarthy I, O'Brien M, Ames C, et al. Incremental cost-effectiveness of adult spinal deformity surgery: observed quality-adjusted life years with surgery compared with predicted quality-adjusted life years without surgery. *Neurosurg Focus*. 2014;*36*(5):E3.
31. Cho SK, Kim YJ, Lenke LG. Proximal Junctional kyphosis following spinal deformity surgery in the pediatric patient. *J Am Acad Orthop Surg*. 2015;*23*(7):408-414.
32. Watanab K, Lenke LG, Bridwell KH, Kim YJ, Koester L, Hensley M. Proximal junctional vertebral fracture in adults after spinal deformity surgery using pedicle screw constructs: analysis of morphological features. *Spine*. 2010;*35*(2):138-145.
33. Hostin R, McCarthy I, O'Brien M, et al. Incidence, mode, and location of acute proximal junctional failures after surgical treatment of adult spinal deformity. *Spine*. 2013;*38*(12):1008-1015.
34. Glattes RC, Bridwell KH, Lenke LG, Kim YJ, Rinella A, Edwards C. Proximal junctional kyphosis in adult spinal deformity following long instrumented posterior spinal fusion: incidence, outcomes, and risk factor analysis. *Spine (Phila. Pa. 1976)*. 2005;*30*(14):1643-1649.
35. Lamartina C, Berjano P. Classification of sagittal imbalance based on spinal alignment and compensatory mechanisms. *Eur Spine J*. 2014;*23*(6):1177-1189.
36. Kim YJ, Bridwell KH, Lenke LG, Glattes CR, Rhim S, Cheh G. Proximal junctional kyphosis in adult spinal deformity after segmental posterior spinal instrumentation and fusion: minimum five-year follow-up. *Spine (Phila. Pa. 1976)*. 2008;*33*(20):2179-2184.
37. Cawley DT, Alexander M, Morris S. Multifidus innervation and muscle assessment post-spinal surgery. *Eur Spine J*. 2014;*23*(2):320-327.
38. Keller A, Gunderson R, Reikerås O, Brox JI. Reliability of computed tomography measurements of paraspinal muscle cross-sectional area and density in patients with chronic low back pain. *Spine (Phila. Pa. 1976)*. 2003;*28*(13):1455-1460.
39. Keller A, Brox JI, Gunderson R, Holm I, Friis A, Reikerås O. Trunk muscle strength, cross-sectional area, and density in patients with chronic low back pain randomized to lumbar fusion or cognitive intervention and exercises. *Spine (Phila pa 1976)*. 2004;*29*(1):3-8.
40. Min S-H, Kim M, Seo J-B, Lee J-Y, Lee D-H. The quantitative analysis of back muscle degeneration after posterior lumbar fusion: comparison of minimally invasive and conventional open surgery. *Asian Spine J*. 2009;*3*(part 2):85-95.

41. Ryuichi G, Hisao M, Yoshiharu K. Serial changes in trunk muscle performance after posterior lumbar surgery. *Spine Diagn*. 1999;*24*(10):1023-1028.
42. Yagi M, Hosogane N, Okada E, et al. Factors affecting the postoperative progression of thoracic kyphosis in surgically treated adult patients with lumbar degenerative scoliosis. *Spine (Phila. Pa. 1976)*. 2014;*39*(8):E521-E528.
43. Ignasiak D, Peteler T, Fekete TF, Haschtmann D, Ferguson SJ. The influence of spinal fusion length on proximal junction biomechanics: a parametric computational study. *Eur Spine J*. 2018;*27*(9):2262-2271.
44. Malakoutian M, Street J, Wilke HJ, Stavness I, Fels S, Oxland T. A musculoskeletal model of the lumbar spine using ArtiSynth–development and validation. *Comput Methods Biomech Biomed Eng Imaging Vis*. 2018;*6*(5):483-490.
45. Pai SA, Zhang H, Shewchuk JR, et al. Quantitative identification and segmentation repeatability of thoracic spinal muscle morphology. *JOR Spine*. 2020;*3*(3):e1103.
46. Fedorov A, Beichel R, Kalpathy-Cramer J, et al. 3D slicer as an image computing platform for the quantitative imaging network. *Magn Reson Imaging*. 2012;*30*:1323-1341.
47. Santaguida L, McGill SM, Stevens J. Measurement of the trunk musculature from T5 to L5 using MRI scans of 15 young males corrected for muscle fibre orientation. *Clin Biomech*. 1993;*8*:171-178.
48. Jorgensen MJ, Marras WS, Granata KP, Wiand JW. MRI-derived moment-arms of the female and male spine loading muscles. *Clin Biomech*. 2001;*16*(3):182-193.
49. Jorgensen MJ, Marras WS, Smith FW, Pope MH. Sagittal plane moment arms of the female lumbar region rectus abdominis in an upright neutral torso posture. *Clin Biomech (Bristol, Avon)*. 2005;*20*(3):242-246. https://doi.org/10.1016/j.clinbiomech.2004.10.009
50. Jorgensen MJ, Marras WS, Gupta P, Waters TR. Effect of torso flexion on the lumbar torso extensor muscle sagittal plane moment arms. *Spine J*. 2003;*3*(5):363-369.
51. Dumas GA, Poulin MJ, Roy B, Gagnon M, Javanovic M. Orientation and moment arms of some trunk muscles, spine. *Spine (Phila. Pa. 1976)*. 1991;*16*(3):293-303.
52. Dumas GA, Poulin MJ, Roy B, Gagnon M, Jovanovic M. Orientation and moment arms of some trunk muscles. *Transplantation*. 1973;*16*(3):293-303.
53. Kumar S. Moment arms of spinal musculature determined from CT scans. *Clin. Biomech*. 1988;*3*(3):137-144.
54. Hwang J, Dufour JS, Knapik GG, et al. Prediction of magnetic resonance imaging-derived trunk muscle geometry with application to spine biomechanical modeling. *Clin Biomech*. 2016;*37*:60-64.
55. Anderson DE, D'Agostino JM, Bruno AG, Manoharan RK, Bouxsein ML. Regressions for estimating muscle parameters in the thoracic and lumbar trunk for use in musculoskeletal modeling. *J Biomech*. 2012;*45*(1):66-75.
56. McGill SM, Santaguida L, Stevens J. Measurement of the trunk musculature from T5 to L5 using MRI scans of 15 young males corrected for muscle fibre orientation. *Clin Biomech*. 1993;*8*:171-178.
57. Susan S, *Gray's Anatomy 41st Edition: The Anatomical Basis of Clinical Practice*. London: 2016.
58. Netter FH. *Atlas of Human Anatomy - Seventh Editing*. Philadelphia, PA: Elsevier-Heal. Sci. Div; 2018.
59. Moore KL, Dalley AF, Agur AMR. *Clinically Oriented Anatomy*. 7th ed. Philadelphia, PA: Wolters Kluwer Health/Lippincott Williams & Wilkins 2014.
60. Lee SHST et al. Changes in activation of serratus anterior, trapezius and latissimus dorsi with slouched posture. *Ann Rehabil Med*. 2016;*40*(2):318-325.
61. Jorgensen MJ, Marras WS, Gupta P. Cross-sectional area of the lumbar back muscles as a function of torso flexion. *Clin Biomech*. 2003;*18*(4):280-286.
62. O'Sullivan PB et al. Effect of different upright sitting postures on spinal-pelvic curvature and trunk muscle activation in a pain-free population. *Spine (Phila. Pa. 1976)*. 2006;*31*(19):E707-12.
63. Ourieff J, Scheckel B, Agarwal A. *Anatomy, Back, Trapezius*. In: StatPearls [Internet]. Treasure Island (FL): StatPearls Publishing; 2020.
64. Macintosh JE, Bogduk N, Pearcy MJ. The effects of flexion on the geometry and actions of the lumbar erector spinae. *Spine*. 1993;*18*(7):884-893.
65. Bojadsen TWA, Silva ES, Rodrigues AJ, Amadio AC. Comparative study of mm. Multifidi in lumbar and thoracic spine. *J Electromyogr Kinesiol*. 2000;*10*(3):143-149.
66. Chaffin DB, Redfern MS, Erig M, Goldstein SA. Lumbar muscle size and locations from CT scans of 96 women of age 40 to 63 years. *Clin Biomech*. 1990;*5*(1):9-16.
67. Tracy MF, Gibson MJ, Szypryt EP, Rutherford A, Corlett EN. The geometry of the muscles of the lumbar spine determined by magnetic resonance imaging. *Spine*. 1989;*14*(2):186-193.
68. Suderman BL, Vasavada AN. Neck muscle moment arms obtained in-vivo from MRI: effect of curved and straight modeled paths. *Ann Biomed Eng*. 2017;*45*(8):2009-2024.
69. Anderson JS, Hsu AW, Vasavada AN. Morphology, architecture, and biomechanics of human cervical multifidus. *Spine (Phila. Pa. 1976)*. 2005;*30*(4):86-91.
70. Vasavada AN, Lasher RA, Meyer TE, Lin DC. Defining and evaluating wrapping surfaces for MRI-derived spinal muscle paths. *J Biomech*. 2008;*41*(7):1450-1457.
71. Burnett A, O'Sullivan P, Caneiro JP, Krug R, Bochmann F, Helgestad GW. An examination of the flexion-relaxation phenomenon in the cervical spine in lumbo-pelvic sitting. *J Electromyogr Kinesiol*. 2009;*19*(4):e229-e236.
72. Hansen L, De Zee M, Rasmussen J, Andersen TB, Wong C, Simonsen EB. Anaatomy and biomechanics of the back muscles in the lumbar spine with reference to biomechanical modeling. *Spine (Phila. Pa. 1976)*. 2006;*31*(17):1888-1899.
73. Banno T, Arima H, Hasegawa T, et al. The effect of paravertebral muscle on the maintenance of upright posture in patients with adult spinal deformity. *Spine Deform*. 2019;*7*(1):125-131.

How to cite this article: Pai S A, Zhang H, Street J, Wilson DR, Brown SHM, Oxland TR. Preliminary investigation of spinal level and postural effects on thoracic muscle morphology with upright open MRI. *JOR Spine*. 2021;4:e1139. https://doi.org/10.1002/jsp2.1139